

End Turn Leakage Reactance of Concentrated Modular Winding Stators

Cox, Tom^{1,2}, Eastham, J Fred¹, Proverbs, J²

¹The University of Bath, Bath, United Kingdom

²Force Engineering, Shephed, United Kingdom

When considering common methods of calculating the end turn reactance of concentrated modular windings, significant effects are seen due to the presence of core iron that are not accounted for in many methods. Experimental study and 3D Finite Element work is carried out to accurately model end turn reactance. A method of accurately predicting end turn reactance with significantly reduced solving and modeling time is developed and tested against experimental results. A parameterized equation is then developed allowing the calculation of end turn reactance for any concentrated modular winding configuration within the proscribed limits. Finally, a method of reducing end turn reactance through the use of concentric coils is developed.

Index Terms –Leakage Inductance, End Turn, Concentrated Winding

I. INTRODUCTION

The common method [1] for calculating end turn inductance of concentrated modular windings involves removing the machine core from the problem and forming air-cored coils from the two end regions of the machine coils. The results of this calculation can vary considerably from the values obtained experimentally due to the presence of the core iron. Lawrenson developed approximate methods for modifying the inductance to allow for the iron in the case of a turbogenerator [2]. It is the objective of this paper to use 3D & 2D finite element modelling to calculate the end turn leakage inductance accurately for concentrated and modular windings, including the presence of the core. These windings are in use for permanent magnet machines [3] and are proposed for special linear induction motors [4].

II. CURRENT ANALYTICAL METHODS

Current literature on end turn leakage inductance for concentrated coils [1] [5] [6] uses a simple method, neglecting the presence of core iron. This method simplifies the racetrack shaped coil structure of Fig. 1a to that of an oval or circle composed purely of the end windings Fig. 1b. This circular end winding section is then solved using conventional inductance formulae.

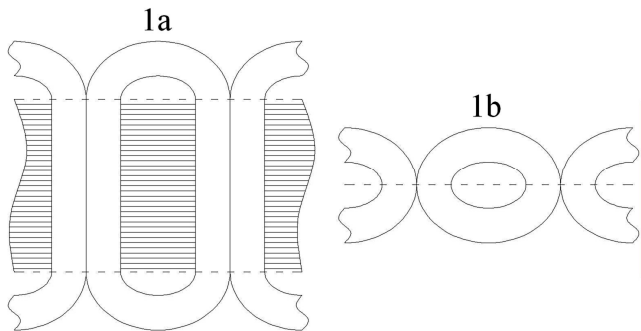


Fig. 1. Simplification of concentrated coil to a circular or oval coil made up of the end sections.

Application of this method to concentrated coil machines showed significant differences between machine inductance calculated using the methods above, and machine inductance measured experimentally.

III. 3D FINITE ELEMENT MODELLING METHODS

To resolve the differences between methods, 3D Finite element modelling using the MEGA package was performed to accurately model the end turn inductance of the concentrated coils. 3 phase sets of coils were used, employing a periodic boundary at each end of the model in order to simulate the behaviour of a true continuous stator. This allowed the model to take into account mutual inductance effects between the end turns of the coils, as well as self inductance effects.

Firstly, 3D finite element models were produced of the simplified end turns as used in the analytical methods described above and the inductance of these was calculated.

A second method of calculating end turn inductance was employed, using several full 3D stator models of varying core widths [7] Fig. 2. For convenience these were linear in form.

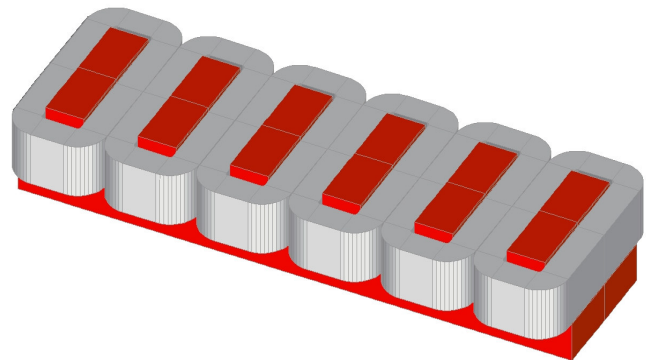


Fig. 2. A 3D Finite Element model of a concentrated winding stator.

The stator inductance measured from the terminals comprises several parts including end turn leakage, slot leakage and magnetising inductance components. It can be shown that whereas all other inductance components are directly proportional to core width, end turn leakage inductance is constant. Therefore, if the terminal inductances of several otherwise identical machines of varying core width are plotted, referring this plot to zero core width will yield a value for end turn leakage inductance per coil as shown in Fig. 3.

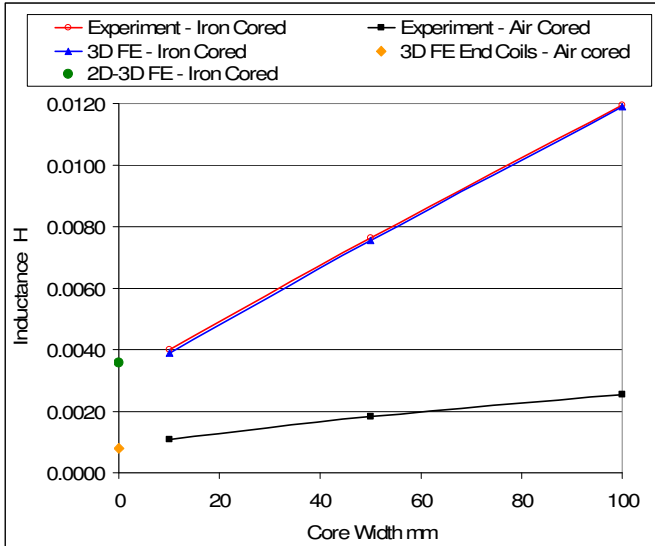


Fig. 3. Experimental results with and without iron core, Iron cored coil 3D FE results, air cored end turn coil (as in Fig. 1) 3D FE results and results of 2D-3D iron cored FE method.

IV. EXPERIMENTAL RESULTS

This method and its results have been validated experimentally, by constructing 3 otherwise identical machines of reducing core width Fig. 4, and referring to zero core width. These results are also plotted on Fig. 3. for comparison with the FE values. It will be observed that the correlation between the results is excellent.



Fig. 4. Experimental concentrated winding linear machines of varying core width, with identical end turn dimensions.

V. DIFFERENCES

The main reason for the differences between experimental and FE results and the simple analytical method [1] is the presence of Iron [2]. The analytical method makes no allowances for the presence of iron, where this has been shown experimentally to have a significant effect on the measured end turn inductance. The three machines of varying core width have been tested experimentally with and without iron cores, and their inductance referenced back to zero Fig. 3. This shows an obvious and significant difference due to the presence of an iron core.

VI. A NEW SIMPLE METHOD

A simpler method has also been developed. A full 3D FE model can accurately model all aspects of a stator, including all inductances. A 2D FE model can accurately model per metre depth all stator characteristics whose parameters can be described in two dimensions, and thus is able to account for all stator inductance effects, with the exception of end turn leakage inductance, which is totally neglected by this method. Therefore, if both 2D and 3D FE models are produced based on the same machine, the difference in inductance between the two must be due mainly to end turn leakage, and can therefore be calculated. This method gave values within 10% of the experimental and full 3D results with significant saving in computation Fig. 3.

VII. ANALYTICAL PARAMETERISED MODELLING METHOD

The new simple method developed reduces the computation time, but generating a solution for the end turn inductance of a given machine still requires significant amounts of FE programming and solve time. Therefore, a simple parameterised equation based method was sought to give quick and easy results for end turn inductance. The parameters of the machine that affected end turn inductance were first defined as shown in Fig. 5.

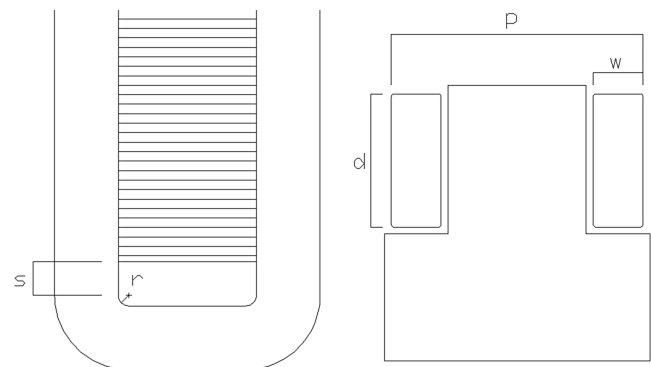


Fig. 5. Relevant coil dimensions for determining end turn inductance of a concentrated coil machine.

The distance between the stack and the inner edge of the coil was fixed, based on the minimum likely clearance from the stack side s (5mm) and the minimum inner bend radius r (2mm). The principal parameters that affect end turn inductance are coil width w , coil depth d and coil pitch p . A useful range of parameters was then defined, suitable for a range of machines usually encountered in practice. Coil width

w was modelled between 10-120mm, coil depth d was modelled between 30-50mm and coil pitch p between 40-280mm.

The 2D and 3D comparison method described above was used to find values of end turn inductance for approximately 100 cases throughout the range of parameters. These values were then used to develop the parameterised equation [8] for inductance per turn (1). Within its designed range, this equation is able to predict the end turn inductance of a machine within 10% of 3D FE results. Despite being relatively large, this equation also gives results in a fraction of the time taken by even the fastest FE solves.

$$L = \left(\begin{aligned} & (+8.190 \times 10^{-21} \times d^2 + 1.252 \times 10^{-18} \times d - 2.611 \times 10^{-17}) \times w^4 + \\ & (-2.036 \times 10^{-18} \times d^2 - 2.824 \times 10^{-16} \times d + 2.217 \times 10^{-15}) \times w^3 + \\ & (+1.765 \times 10^{-16} \times d^2 + 2.207 \times 10^{-14} \times d + 2.380 \times 10^{-13}) \times w^2 + \\ & (-7.875 \times 10^{-15} \times d^2 - 5.620 \times 10^{-13} \times d - 3.234 \times 10^{-11}) \times w + \\ & (+2.045 \times 10^{-13} \times d^2 + 3.095 \times 10^{-12} \times d + 2.581 \times 10^{-09}) \end{aligned} \right) \times p$$

$$+ \left(\begin{aligned} & (-2.180 \times 10^{-18} \times d^2 + 2.430 \times 10^{-16} \times d + 6.477 \times 10^{-15}) \times w^4 + \\ & (+4.415 \times 10^{-16} \times d^2 - 6.377 \times 10^{-14} \times d - 1.006 \times 10^{-12}) \times w^3 + \\ & (-2.495 \times 10^{-14} \times d^2 + 5.292 \times 10^{-12} \times d + 5.193 \times 10^{-11}) \times w^2 + \\ & (+5.600 \times 10^{-13} \times d^2 - 2.045 \times 10^{-10} \times d - 2.531 \times 10^{-09}) \times w + \\ & (-1.079 \times 10^{-11} \times d^2 + 4.295 \times 10^{-09} \times d - 3.359 \times 10^{-08}) \end{aligned} \right) \quad (1)$$

VIII. CONCENTRIC CONCENTRATED WINDING STATORS

A method has also been investigated to reduce the effects of end turn leakage inductance by moving from single concentrated coils as in Fig. 2 to two or more concentrically wound distributed coils as in Fig. 6.

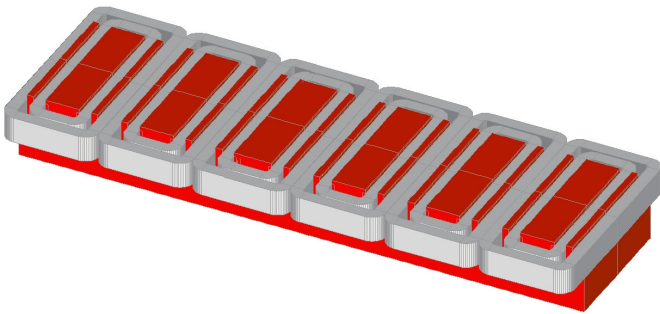


Fig. 6. Dual coil concentric winding 3D FE model.

This has the effect of dramatically reducing the self inductance of each coil, whilst including some mutual coupling between the two coils, based on the separation and dimensions of the pair. With careful design, a configuration such as this can significantly reduce the overall end turn inductance of a stator.

The end turn inductance of these concentric groups can be modelled using the 2D-3D method described above, and may be parameterised using the methods previously described.

Starting from a concentrated coil machine as in Fig. 5, each coil is divided into two concentric coils as shown in Fig. 7. The coil depth of the new coils is still d , the offset from stack

for the inner coil is still s and the bend radius is still r . The coil width for each concentric is now $\frac{1}{2}w$. The tooth width between the coils t can take any value. The coil pitch of the outer coil is still p and the coil pitch of the inner coil p_2 is equal to $p - w - 2t$.

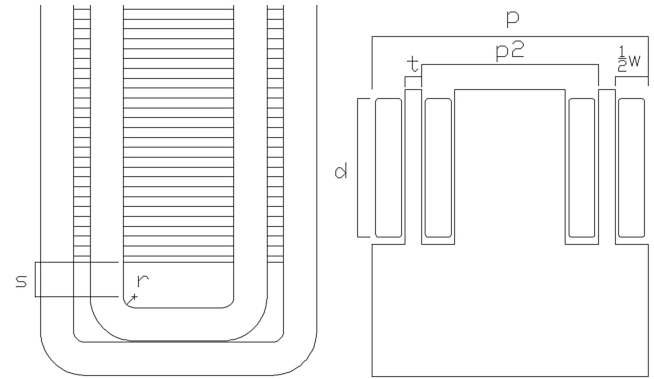


Fig. 7. Coil dimensions for determining end turn inductance of a 2 coil concentric machine.

An example case is detailed below.

The original coil had the following characteristics: Coil pitch p 71.2mm, coil width w 20.8 mm, coil depth d 37mm, offset from stack s 5mm and bend radius r 2mm.

The end turn inductance per coil of this machine found from both 3 core full 3D FE and experiment was 0.0032H.

The method detailed in this section was used to develop a 2 coil concentric equivalent machine. The characteristics of this were: Outer coil pitch p 71.2mm, inner coil pitch p_2 40.4mm, inter-coil tooth width t 5mm, coil width $\frac{1}{2}w$ 10.4 mm, coil depth d 37mm, offset from stack s 5mm and bend radius r 2mm.

The end turn inductance per coil of this machine, using 3 core results for full 3D FE was 0.00195H, a reduction in end turn inductance of 40%.

A significant variable in the 2 coil concentric method is inter-coil tooth width t . The greater this value is the less mutual inductance there will be between the two concentric coils and the better the end turn inductance will be. However, splitting the coil into two concentrics also reduces performance by adding a distribution factor to the overall winding factor, hence reducing it. This distribution factor is related to concentric coil separation and hence inter-coil tooth width t .

In practice, there is a delicate balance to be found between reducing end turn inductance and limiting the reduction of winding factor in order to produce an overall improvement using this method.

IX. CONCLUSIONS

Simple analytical methods of end turn leakage inductance modelling have been found to be inexact when modelling planar concentrated iron cored coils. The improved method developed has resulted in a fast and accurate equation for calculating end turn inductance that can be solved extremely quickly with modern computer systems. The correlation between experimental results and 2D finite element results using this method of calculating end turn inductance is excellent. The final figure Fig. 8. shows the force speed curve of an offset concentrated winding machine firstly modelled

with 2D finite elements using the equation developed above to predict end turn inductance, then with finite elements using a value of end turn inductance based on the simple air cored coil method, and finally measured experimentally using a standstill variable frequency method [9].

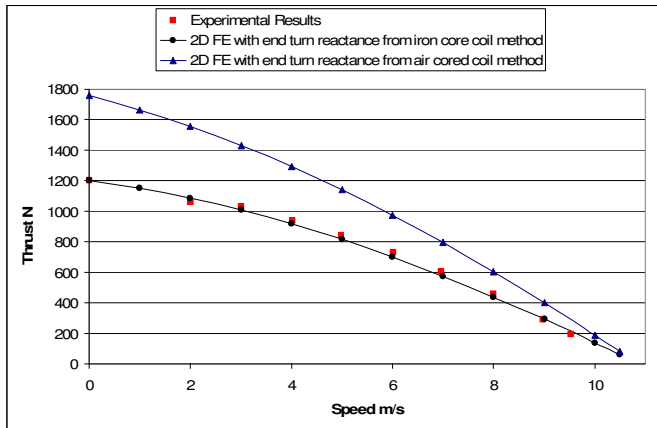


Fig. 8. Force Speed curve showing experimental and 2D finite element results.

It must be noted that although in this case the end turn inductance makes a significant difference to the overall results, the end turn inductance in terms of overall inductance is relatively large in this type of linear machine, due to the relatively narrow core width. In machines of greater core width, other inductances become dominant and the effect of errors in end turn inductance is much less apparent. For example, for the machine of Fig. 8 with a 100mm core width the error in stall thrust due to an incorrect end turn inductance value is 46%. With a 500mm core width the error in the same machine due to incorrect end turn inductance is now only 10%.

APPENDIX

FINITE ELEMENT MODELLING

The 2D and 3D finite element analysis (FE) documented in this paper was undertaken using the University of Bath MEGA software.

Electromagnetic fields can be modeled using the magnetic vector potential, \mathbf{A} . The governing equation is:

$$\nabla \times \frac{1}{\mu} \nabla \times \mathbf{A} + \sigma \frac{\partial \mathbf{A}}{\partial t} = \mathbf{J} \quad (2)$$

where:

μ is the permeability in henries/meter

\mathbf{A} is the magnetic vector potential in webers/metre

σ is the conductivity in siemens/metre

By using the finite element method together with the Galerkin weighted residual procedure this can be transformed into a system of equations.

For the modeling of force at a particular plate velocity as seen in Fig. 7, a Minkowski transform was used to simulate the effects of a rotor of constant cross sectional area moving at constant velocity past a pair of offset short stators [4]. This technique removes the need for full time-stepped solutions, allowing simpler and faster solution of each velocity point without compromising accuracy.

The Russell & Norsworthy Factor was used to modify the rotor resistivity in order to simulate the secondary end ring effects [10].

A view of the stator and rotor mesh that was used is shown in Fig. 9.

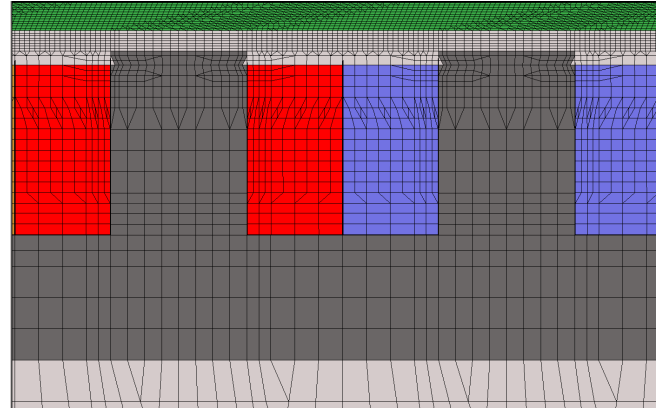


Fig. 9. The finite element stator and rotor mesh used in the models.

ACKNOWLEDGMENT

This work was undertaken as part of a Knowledge Transfer Partnership supported by the Technology Strategy Board, UK

REFERENCES

- [1] Hendershot, J. R. Jr. and Miller T.J.E 'Design of brushless permanent-magnet motors' Magna Physics Publishing & Clarendon Press Oxford 1994.
- [2] Lawrenson, P. J. 'Calculation of machine end-winding inductances with special reference to turbogenerators' Proc IEE Vol. 117, No.6, June 1970.
- [3] J Wang, Z P Xia, D Howe, S A Long, "Comparative Study of 3-Phase Permanent Magnet Brushless Machines with Concentrated, Distributed and Modular Windings" IET Power Electronics, Machines and Drives, Mar. 2006 Page(s):489 - 493
- [4] J.F Eastham, T Cox, H.C Lai, J Proverbs, "The use of concentrated windings for offset double stator linear induction motors", LDIA Lille Sep. 2007
- [5] Grover, F.W.: 'Inductance calculations' Dover Publications, New York, 1946
- [6] Liwshitz-Garik, M.: 'Electric machinery, Vol. 1, Fundamental and DC machines' D. Van Nostrand Company, Toronto, 1946
- [7] Barnes, E.C., 'An experimental study of induction machine end-turn leakage reactance', AIEE Trans., Vol 70, 1951, pp671-679
- [8] Hamlaoui M.N., Mueller M.A., Bumby J.R., Spooner E., 'Polynomial modelling of electromechanical devices: an efficient alternative to look up tables', IEE Proc.-Electr. Power Appl., Vol 151, No. 6, Nov. 2004
- [9] J F Eastham, P C Coles, M Benarous, J Proverbs, A Foster "Linear Induction Motor Variable Frequency Standstill Tests to Predict Operational Velocity Performance" LDIA 2003 Birmingham, UK pp 81-84
- [10] Russell, R.L. and Norsworthy, K H. "Eddy Current and Wall Losses in Screened Rotor Induction Motors" Proc. I.E.E. Paper No. 2525 U, Apr 1958 (105 A, 163)